Int. J. Electrochem. Sci., 10 **(2015)** 373 - 387

International Journal of
ELECTROCHEMICAL
SCIENCE
www.electrochemsci.org

Fabrication of Different Protective Coatings and Studying their Mechanical Properties and Corrosion Behavior in Sodium Chloride Solutions

El-Sayed M. Sherif[1,2,*], *Mohammad Asif Alam*[1], *Saeed M. Al-Zahrani*[1,3]

[1] Center of Excellence for Research in Engineering Materials (CEREM), Advanced Manufacturing Institute, King Saud University, P. O. Box 800, Al-Riyadh 11421, Saudi Arabia
[2] Electrochemistry and Corrosion Laboratory, Department of Physical Chemistry, National Research Centre (NRC), Dokki, 12622 Cairo, Egypt
[3] SABIC Polymer Research Center (SPRC), Department of Chemical Engineering, College of Engineering, King Saud University, P.O. Box 800, Al-Riyadh 11421, Saudi Arabia
[*]E-mail: esherif@ksu.edu.sa; emsherif@gmail.com

Received: 3 September 2014 / *Accepted:* 28 October 2014 / *Published:* 2 December 2014

Five formulations of protective coatings were fabricated by treating bisphenol based epoxy resin A (BBERA) with different stoichiometry variations of polyaminoamine 115-Cray valley (PAA-115) as a hardener at ambient temperature. The fabricated epoxy coatings were first applied on glass plates for studying their mechanical properties. Other portions of the coatings were applied on steel substrates for reporting the corrosion behavior in an aerated 0.6 M NaCl solution. The chemical composition of the fabricated formulations was characterized using Fourier-transform infrared spectroscopy (FT-IR). A differential scanning calorimetry was used to report the thermal degradation of the fabricated coatings. The mechanical properties for the different coatings were evaluated using various techniques such as cross hatch tester, pendulum hardness, mandrel bend, and scratch tester measurements. The corrosion behavior for all coated steels after 60 min and 7.0 days immersion in 0.6 M NaCl solutions was performed using electrochemical impedance spectroscopy (EIS) investigations. It has been found that the five fabricated coatings provide high thermal stability, excellent mechanical properties and good corrosion behavior and their corrosion resistance decreased with increasing the exposure time from 60 min to 7.0 days before measurement.

Keywords: bisphenol-A epoxy resin; corrosion; EIS; protective coatings, mechanical properties

1. INTRODUCTION

Organic coatings have been widely used as the first line defines in the protection metals and alloys against corrosion and wear in aggressive media [1-5]. Corrosion and wear resistant coatings

have been employed in various industries such as in defense, power generation, magnetic storage devices and bearings, utility, automobile, engine parts and seals, aerospace, optical equipment [6-9]. This type is called a protective coating and must be characterized by its high barrier and excellent mechanical properties. Moreover, it imparts specific engineering properties of a substrate material by modifying or applying a thin layer at its surface. From this point of view, the driving force for the advancement in the industry of coatings has been an improvement in corrosion and wear resistances. This is to improve the performance and reliability for coatings in order to resist various types of corrosion such as uniform, pitting, crevice, and exfoliation, as well as erosion, sliding and wear [1-4].

Coatings applied at the time of manufacture of products are known as industrial coatings. Many industrial coating processes involve the application of a thin film of functional material to a substrate, such as paper, fabric, film, foil, or sheet stock. Coatings may also be applied on surfaces where immersion is not continuous such as the external surfaces of tanks and pipes [4]. Although there have been several coatings like vinyl based coatings, acrylic coatings, polyurethane coatings, etc, available in the market, epoxy coatings system plays a vital role in marine coating industries [10]. P. Kalenda [11] has reported that the molecular weight of the epoxy resin and concentration of the employed curing agent affect the performance of any epoxy curing system. There are many curing agents have been widely used for epoxy applications; some of these are polyamidoamine, polyamine, and polyamide, in addition to several other several agents [1-4]. For that the producers of epoxy coatings frequently examine and identify their coatings with a unique combination of epoxy resin and curing agent.

It is well know that one of the most effective ways to prevent corrosion is the use of protective coatings. The use of coatings in protecting metallic structures has been reported by numerous investigators [1,4,12-14]. In order for a coating to provide adequate corrosion protection, the coating must be uniform, well adhered, pore free and self-healing for applications where physical damage to the coating may occur [12]. It has been also reported [11,12,15,16] that there are different mechanisms employed in protecting metals and alloys using protective coatings; some of these are, providing a barrier between the metal and its environment isolating the metal from being attacked by its environment and/or through the presence of corrosion inhibiting chemicals within the coating, a sacrificial metal coating that corrodes while giving cathodic protection to the base metal, a noble metal coating that ensures that the base metal is in the passive state, an electrically resistive coating that slows down electrochemical corrosion reactions, etc.

We have been studying the corrosion and corrosion protection of metals and alloys in aggressive media using organic coatings [1,4,17,18]. Our previous work [1], reported the fabrication of various epoxy coatings using bisphenol-A diglycidyl ether epoxy resin (DGEBA) that was treated with different stoichiometry variations of polyamidoamine adducts (ARADUR-PA450) as a curing agent for offshore applications. Moreover, we synthesized a different series of epoxy coatings from diglycidyl ether of bisphenol-A (DGEBA) epoxy resin that was cured by physical mixing with Aradur®-3282 polyamidoamine adducts (Aradur®-PA3282) as a curing agent [4]. The mechanical properties as well as the corrosion behavior for all of the fabricated coatings were also reported. It has been found that these coatings have superior mechanical properties and can be used as protective

coatings against corrosion in marine environments due to the high cross-linking of the amino group of the polyamidoamine adducts ARADUR 450 and Aradur®-3282 at ambient temperature [1,4].

The current work aims at fabricating of various epoxy coating formulations using bisphenol based epoxy resin A (BBERA) and an optimized quantity of polyaminoamine 115-Cray valley (PAA-115) as a hardener at ambient temperature. This was to obtain high performance for corrosion resistance applications. The optimization was performed based on the different stoichiometric ratios of the PAA-115 curing agent. Different characterization procedures were employed to evaluate the mechanical properties of the fabricated coatings such as pendulum hardness, scratch test, mandrel bend test, cross hatch test, and FTIR-ATR techniques. The corrosion resistance after 60 min and 7.0 days immersion in freely aerated stagnant 0.6 M NaCl solutions at room temperature was tested using electrochemical impedance spectroscopy.

2. EXPERIMENTAL DETAILS

2.1. Chemicals and materials

Bisphenol based epoxy resin A (BBERA, Hexion Chemicals), polyaminoamine 115-Cray valley hardener, (PAA115, Huntsman Advanced Materials), acetone (Merck, 99%), methyl isobutyl ketone (MIBK, Merck), xylene (Merck, 99%), and an air releasing agent. The different coatings were applied on both glass and steel plates as substrates in order to perform the different characterization measurements. Corrosion measurements were carried out in a freely aerated stagnant solution of 0.6 M sodium chloride (NaCl, Merck, 99%).

2.2. Fourier-transform infrared spectroscopy (FTIR-ATR) investigation

FTIR-ATR spectra were recorded for the different coatings formulations on a Perkin-Elmer infrared spectrophotometer 1720X equipped with a liquid nitrogen-cooled mercury-cadmium-telluride detector.

2.3. Thermal degradation analysis

A differential scanning calorimetry (DSC, Shimadzu DSC60) was used to thermally characterize the coatings under consideration. The procedures used to thermally characterize the current epoxy coatings have been reported in our previous work [1].

2.4. Mechanical properties measurements

Koenig hardness was measured using pendulum hardness rocker (Sheen Instruments Co., UK). The thickness of the film applied on the surface of the glass and steel plates was measured using an Ecotest plus instrument (Sheen Instruments Co., UK). The scratch, flexibility and adhesion

measurements were carried out using scratch tester, mandrel bend and cross hatch testers (Sheen Instruments Co., UK), respectively.

2.5. Electrochemical impedance spectroscopy (EIS) measurements

EIS experiments were performed by using an Autolab Potentiostat (PGSTAT20 computer controlled) operated by the general purpose electrochemical software (GPES) version 4.9. An electrochemical cell with a three-electrode configuration was used; a coated steel, a stainless steel, and an Ag/AgCl electrode (in saturated KCl solution), were used as the working, counter, and reference electrodes, respectively. EIS Nyquist and Bode plots were collected at the corrosion potential after immersing the coated samples for 60 min and 7.0 days in 0.6 M NaCl solution. The scanned frequency range was between 10,000 Hz and 0.01 Hz, an ac wave of ± 5 mV peak-to-peak overlaid on a dc bias potential, and the impedance data were collected using Powersine software at a rate of 10 points per decade change in frequency. All measurements were carried out at room temperature using two samples to obtain statistically significant results.

3. RESULTS AND DISCUSSION

3.1. Fabrication of different BBERA-PAA115 epoxy coatings

Table 1. The weight percentages of the chemicals used to obtain the different BBERA-PA115 formulations

Formula	PAA-115 hardener	BBERA	Xylene	MIBK	Air releasing agent	Stoichiometry
F-1	45.49	14.31	20	20	0.2	+20
F-2	41.70	18.10	20	20	0.2	+10
F-3	37.91	21.89	20	20	0.2	0.0
F-4	34.11	25.69	20	20	0.2	-10
F-5	30.32	29.48	20	20	0.2	-20

Different formulations of epoxy coatings were fabricated by mixing up varied percentages of BBERA resin with different additives of PAA-115 as a hardener. These formulations were prepared by stirring a considerable amount of BBERA resin at 500 rpm in a dispermat mixer (BYK Gardener, Germany) for 5 min; to this the MIBK and xylene were gradually added at the same speed. The air releasing agent was drop by drop added during the initial mixing period to achieve homogeneous mixing with the organic solvents. The hardener, PAA-115 was at last added to the mixture and all the sizes were thoroughly stirred at 1000 rpm. The obtained coatings were then applied on glass and steel plates to be employed in the different mechanical and electrochemical tests. The steel substrates for electrochemical measurements were first ground using different sizes of emery papers and then rinsed

with acetone before drying using nitrogen gas. The film applicator was used to form the epoxy coatings film on the steel substrates and then they were left to dry at room temperature. The weight percentages of the chemicals used to obtain the different BBERA-PA115 formulations are shown in Table 1.

3.2. Fourier-transform infrared spectroscopy (FTIR-ATR) investigations

The FTIR-ATR investigations were carried out to confirm that the epoxy coatings (BBERA) and the curing agent (PAA-115**)** had homogenious dispersions at the different stoichiometric variations, as well as to characterize the compositions of the fabricated coatings through identifying their functional groups. The FTIR-ATR spectra obtained from the dry glass coated surfaces of F-1, F-2, F-3, F-4, and F-5 epoxy coatings at a wavenumber range from 400 to 1800 cm^{-1}, and are shown in Fig. 1. The FTIR-ATR spectra were also collected for the same surfaces at wavenumber range varied from 1800 to 4000 cm^{-1} as depicted in Fig. 2. The spectra were collected at this wide wavenumber range to ensure the obtaining the reflectance for every spectrum appeared from the surface of the different epoxy formula. According to the previous work [1], the chemical structure of the bisphenol based epoxy resin A (BBERA) molecule contains variety of organic groups such as aromatic rings, -CH3, ≡C-O-C≡, etc. A combination of DGEBA and polyaminoamine 115-Cray valley (PAA-115), which has multi functional groups of -OH, -NH2, -N=N-, =C=O, etc in its molecule, with different stoichiometric variations will compose a compound that contains all of their aromatic and aliphatic groups. The spectra appear from Fig. 1 show different peaks, some of them are; 768, 827, 874, 1007, 1107, 1182, 1239, 1458, 1509, 1606, and 1645 cm^{-1}. For example, the appearance of the peaks at 1400-1000, 1508, and 1606 cm^{-1} is due to the presence of aromatic rings [19-21]. Also, the C-H out-of-plane deformation vibration bands at 768 and 827 cm^{-1} refer to the ring vibrations [1,20,21].

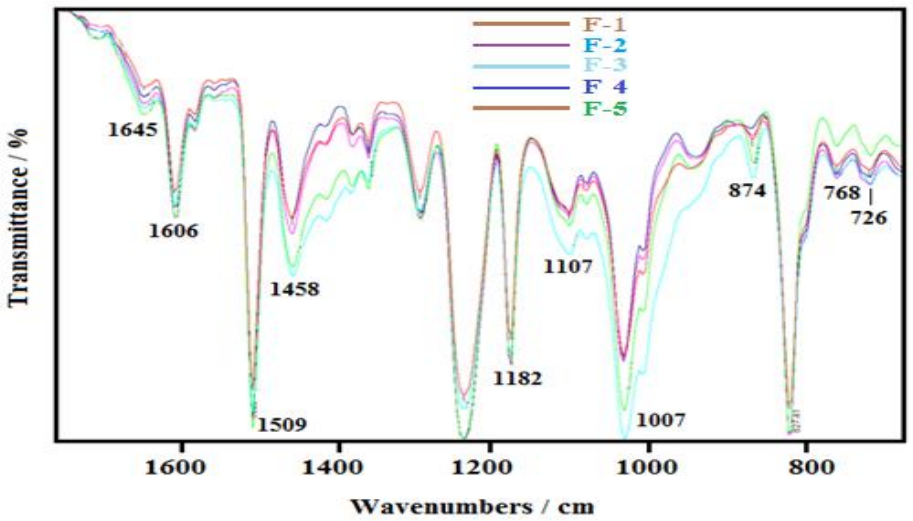

Figure 1. FTIR-ATR spectra obtained over a wavenumber range between 500 and 1800 cm^{-1} for the dry surfaces of F-1, F-2, F-3, F-4, and F-5 epoxy coatings.

Fig. 2 also shows many peaks, namely; 2360, 2850, 2920, 3037, 3308 and 3727 cm^{-1}. The peaks appear between the wavenumber of 2800 and 3050 cm^{-1} have resulted from the presence of aromatic rings [19-21]. While, the broad band between 3200 and 3500 cm^{-1} is mainly due to the presence of O-H stretching of hydroxyl groups [20]. The formation of these hydroxyl groups gives good indications on the formation of epoxy coatings consist of both BBERA and PAA-115 molecules [21]. The increase of the intensity of the spectra seen in Fig. 1 and Fig. 2 is due to the increase of the stoichiometric variation seen in Table 1. Where, the intensity of the spectrum refers to F-5 is higher than the intensity of the spectrum obtained for F-1 epoxy coating. The FTIR-ATR investigations thus proved that the stoichiometric variation controls the composition of the different fabricated BBERA–PAA115 formulations.

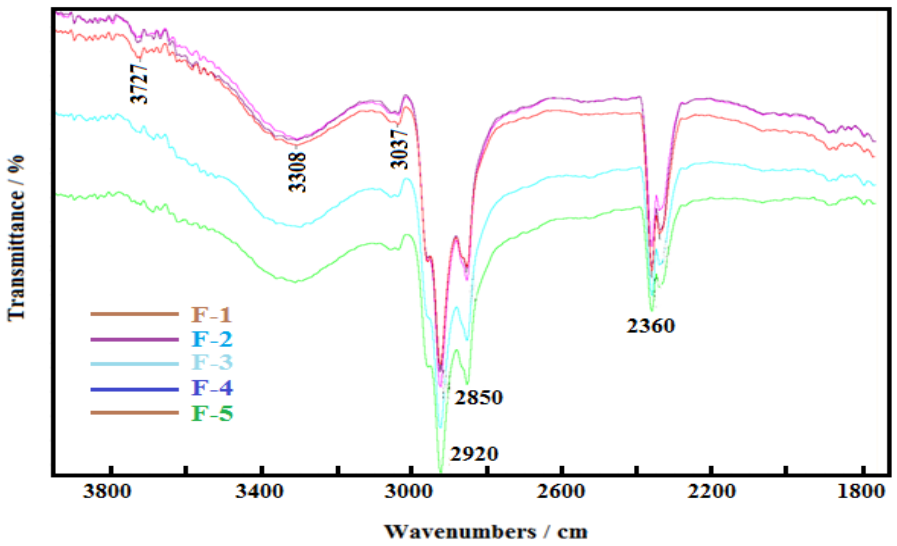

Figure 2. FTIR-ATR spectra obtained over a wavenumber range between 1800 and 4000 cm^{-1} for the dry surfaces of F-1, F-2, F-3, F-4, and F-5 epoxy coatings.

3.3. TGA analysis and SEM investigations

Fig. 3 shows the recorded change in the differential scanning calorimetry (DSC) with increasing temperature (Temp) for the different fabricated BBERA-PAA115 epoxy coatings. A DSC is a thermoanalytical technique from which the difference in the amount of heat required to increase the temperature of a sample and reference is measured as a function of temperature. Our DSC investigations depicted that the main glass transition temperature (TG) for F-1 epoxy coating formula had an amount of 50.35 ºC. Increasing the stoichiometric variation that fits the formation of F-2 epoxy coating sample led to increasing the TG value to 51.70 ºC. Further changes in the TG values were also recorded with changing the stoichiometric variation, where the TG values obtained for F-3, F-4, and F-5 were 49.33 ºC, 50.84 ºC, and 54.43 ºC, respectively.

It has been reported [4] that the high TG value is the better physical interaction between the curing agent and the epoxy resin moieties. In this case the highest TG value was recorded for F-5 epoxy coating sample, which means that the physical interaction between the polyamide (PAA-115)

hardener and the BBERA epoxy resin moieties was the best at the stoichiometric variations equivalent to F-5. The thermal degradation results indicated that the measured TG value for the different fabricated epoxy coatings decreases in the following order; F-3 < F-1 < F-4 < F-2 < F-5. This was confirmed by the SEM micrographs that were obtained on the surface of (a) F-1, (b) F-2, (c) F-3, and (d) F-5 epoxy coatings, which are shown respectively in Fig. 4.

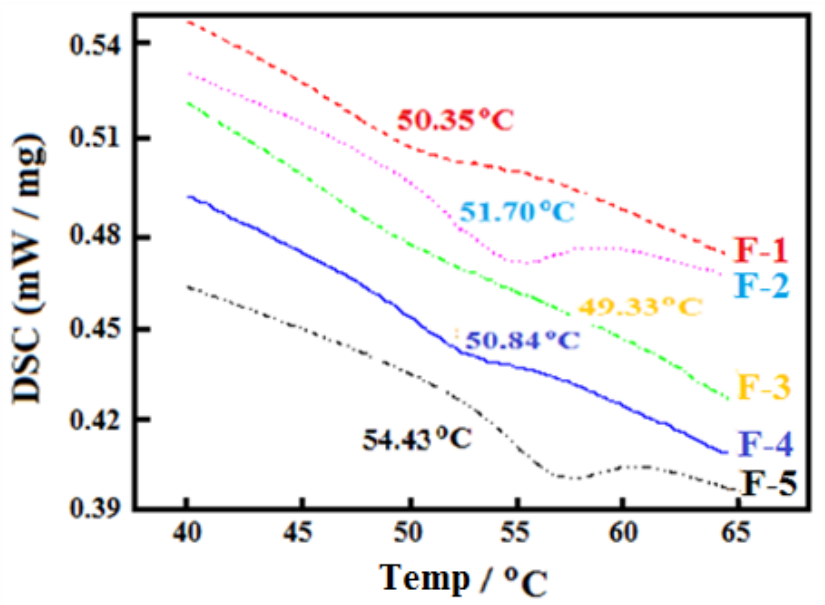

Figure 3. Variation of DSC (mW/mg) with changing temperature (ºC) for the investigated coating formulations.

It is clearly seen from Fig. 4 that the obtained micrographs differ in their surface morphologies from each other depending on the stoichiometric variations between the epoxy resin and hardener. Where, the SEM image of F-5 epoxy coating, Fig. 4 (d) shows the most smooth and homogenious surface, which is most probably due to the better physical interaction between the polyamide (PAA-115) hardener and the BBERA resin moieties. Both TGA and SEM results thus confirm that the stoichiometric variations corresponding to F-5 epoxy coating formula is the best amongst all the fabricated samples.

3.4. Mechanical properties of the epoxy coatings

The mechanical properties of the fabricated formulas of the BBERA-PAA115 epoxy coatings were characterized using different techniques such as dry film thickness, scratch resistance load, Koenig hardness, mandrel bend, and cross hatch tests. The values obtained from all these measurements for the different fabricated epoxy coatings are listed in Table 2. The dry film thickness for all samples was varied between 60 and 70 µm after applying it on glass substrates. The scratch resistant properties of the BBERA-PAA115 epoxy coatings were determined with a dry film thickness of 60-70 µm (Table 2) on steel substrates. The highest scratch resistance for the different formulas was

recorded for the epoxy coating F-1 due to the presence of the polar hydroxyls and oxirane moieties in the backbone of the polymeric chain of the BBERA epoxy resin [1]. The scratch resistance decreased with increasing the stoichiometric variation in the order F-1 > F-2 > F-3 > F-4, while increased slightly again for F-5. This indicates that the decrease of the stoichiometric variation between BBERA epoxy resin and PAA-115 hardener decreases the scratch resistance for the BBERA-PAA115 coating.

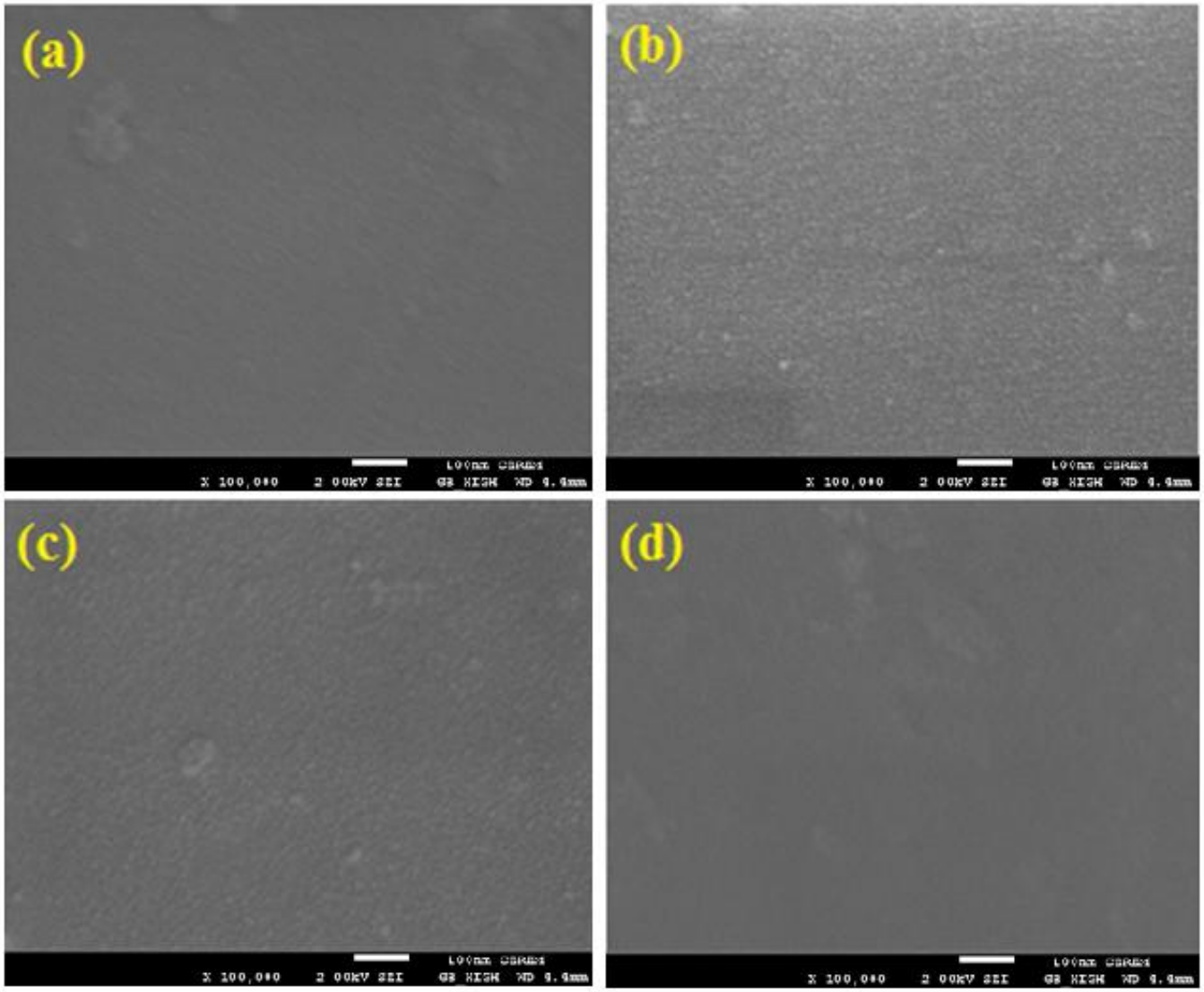

Figure 4. SEM micrographs that were taken for the surface of the epoxy coatings, (a) F-1, (b) F-2, (c) F-3, and (d) F-5, respectively.

Koenig hardness of BBERA-PAA115 epoxy coatings at the stoichiometric variations listed in Table 1 was determined by a dry film thickness of 60-70 μm on glass substrates. ASTM standards for determining the Koenig hardness of epoxy coatings recommend that there should be a layer of at least 25 μm thicknesses required in order to avoid the interference with the substrate [4]. Koenig hardness recorded the highest value for the F-3 epoxy coating sample, which was obtained at 0.0 stoichiometric variations. Table 2 shows that the value of Koenig hardness decreases whether the stoichiometric

variations increase to +10 (F-2) and +20 (F-1) or decrease to -10 (F-4) and -20 (F-5). According to Bhattacharya et al. [22], the hardness value for an epoxy coating is directly related to the proportion of cross-linking between epoxide groups and curing agents. It is worth mentioning that all the fabricated epoxy coatings passed the mandrel bend test perfectly as well as had an excellent Cross-hatch test as can be seen in Table 2. The fabricated BBERA-PAA115 epoxy coatings thus have good mechanical properties at all reported stoichiometric variations between the BBERA epoxy resin and the PAA-115 curing agent.

Table 2. Dry film thickness, scratch resistance load, Koenig hardness, mandrel bend, and cross hatch tests for the different BBERA-PA115 epoxy coatings.

Formula	**Measuring test**				
	Dry film thickness (μm)	Scratch resistance load @ mar failure (kg)	Koenig hardness after 15 days	Mandrel bend test	Cross hatch test
F-1	60 – 70	6.0	117	Pass	Excellent
F-2	60 – 70	4.5	122	Pass	Excellent
F-3	60 – 70	4.0	123	Pass	Excellent
F-4	60 – 70	4.0	121	Pass	Excellent
F-5	60 – 70	5.0	110	Pass	Excellent

3.5. Electrochemical impedance spectroscopy (EIS) investigations

EIS method have been employed in our previous work [1,4,17,18] to report the kinetic parameters for electron transfer reactions at the interface of the coated coupons and corrosive test solution. The technique has also been successfully used to explain the corrosion and corrosion protection mechanisms for metals and alloys in different aggressive environments [23-27]. EIS Nyquist plots obtained for the epoxy coatings, (a) F-1, (b) F-2, (c) F-3, (d) F-4, and (e) F-5 after their immersion in freely aerated 0.6 M NaCl solutions for 60 min and 7.0 days are shown in Fig. 5 and Fig. 6, respectively. These EIS data were fitted to the best equivalent circuit model as shown in Fig. 7; this circuit were also used to fit the EIS data obtained for other epoxy coatings [1,4].. The symbols shown in the circuit are defined as following; R_S is the solution resistance between coated steel coupons and the counter (stainless steel) electrode, Q_1 and Q_2 are the constant phase elements (CPEs), R_{P1} is the resistance of a film layer formed on the surface of the coated coupons, and R_{P2} accounts for the polarization resistance at the coated coupons surface. Moreover, the values of the parameters obtained by fitting the equivalent circuit shown in Fig. 7 are recorded in Table 3.

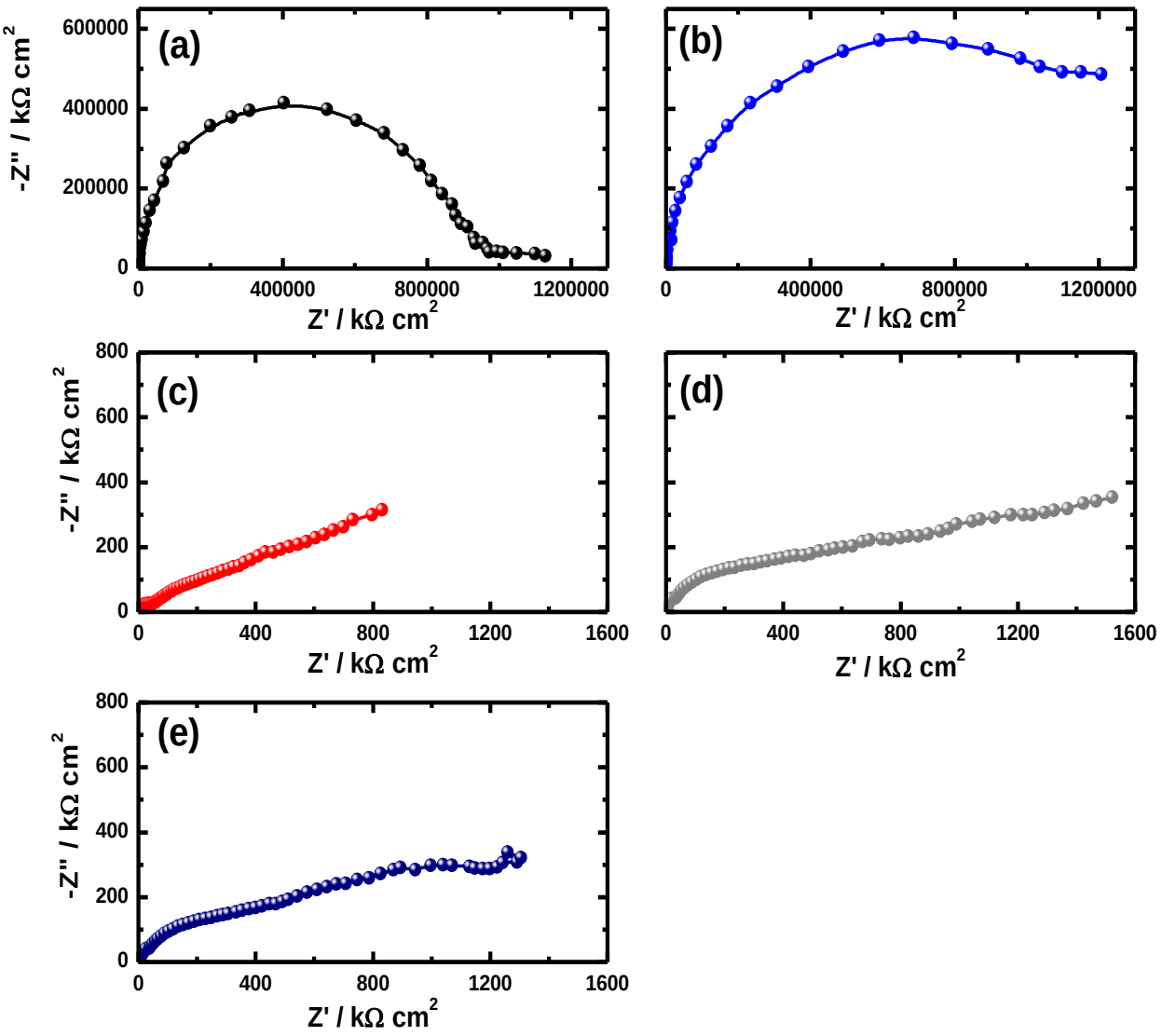

Figure 5. Typical Nyquist plots for the epoxy coatings, (a) F-1, (b) F-2, (c) F-3, (d) F-4, and (e) F-5, respectively after their immersion for 60 min in freely aerated 0.6 M NaCl solutions.

It is clearly seen from Fig. 5 and Fig. 6 that all coated steel electrodes show only one single semicircle followed by a segment; the bigger diameter of the obtained semicircle as well as the larger the segment, the higher the corrosion resistance of the coated surface. It has been reported [28,29] that the diameters of the semicircles at high frequency region can be considered as the charge transfer resistance and the semicircles at high frequencies are generally associated with the relaxation of electrical double layer capacitors. It is also seen that F-2 coupon had the biggest diameter, while F-3 formula had the smallest one for coated electrodes after 60 min immersion in 0.6 M NaCl solution, Fig. 5. In this case, the size of the diameter as well as the corrosion resistance were noticed to decrease in the following order; F-2 > F-1 > F-4 > F-5 > F-3. This was also confirmed by the data listed in Table 3, where R_S, R_{P1} and R_{P2} recorded the highest values for F-2 epoxy coating coupon and the lowest values were for F-3 one.

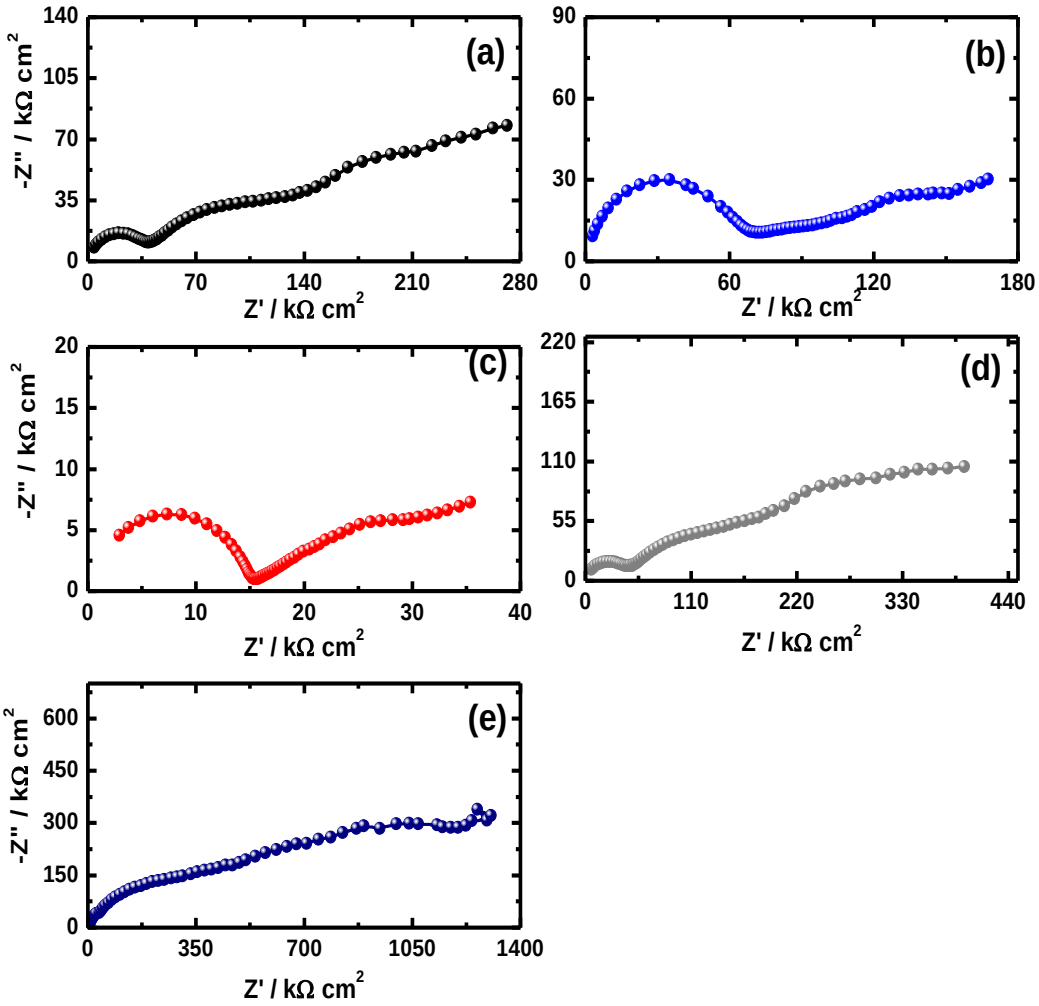

Figure 6. Nyquist plots for the epoxy coatings, (a) F-1, (b) F-2, (c) F-3, (d) F-4, and (e) F-5, respectively after their immersion for 7.0 days in freely aerated 0.6 M NaCl solutions.

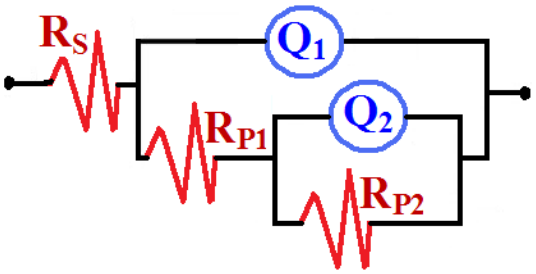

Figure 7. The equivalent circuit model used to fit the experimental data shown in Fig. 5 and Fig. 6.

Table 3 also shows that the CPEs, Q_1 with its n values near to 1.0 represent double layer capacitors with some pores to cover up the charged surfaces [19]. Also, the CPEs, Q_2 with its n value relatively close to 0.5 represent Warburg (W) impedance, which reveals the prevention of dissolution or degradation in the top coating layer through mass transfer. The values recorded of CPEs, Y_{Q1} and Y_{Q2}, were the lowest for F-2 coupon and that further confirms that F-2 had the best performance amongst all fabricated epoxy coatings after their immersion in the chloride solution for 60 min. This indicates that the stoichiometric variation between BBERA and PAA-115 corresponding to F-2 sample

was more compact and adherent to the steel substrate as well as the best in decreasing the flawed and active areas on its surface.

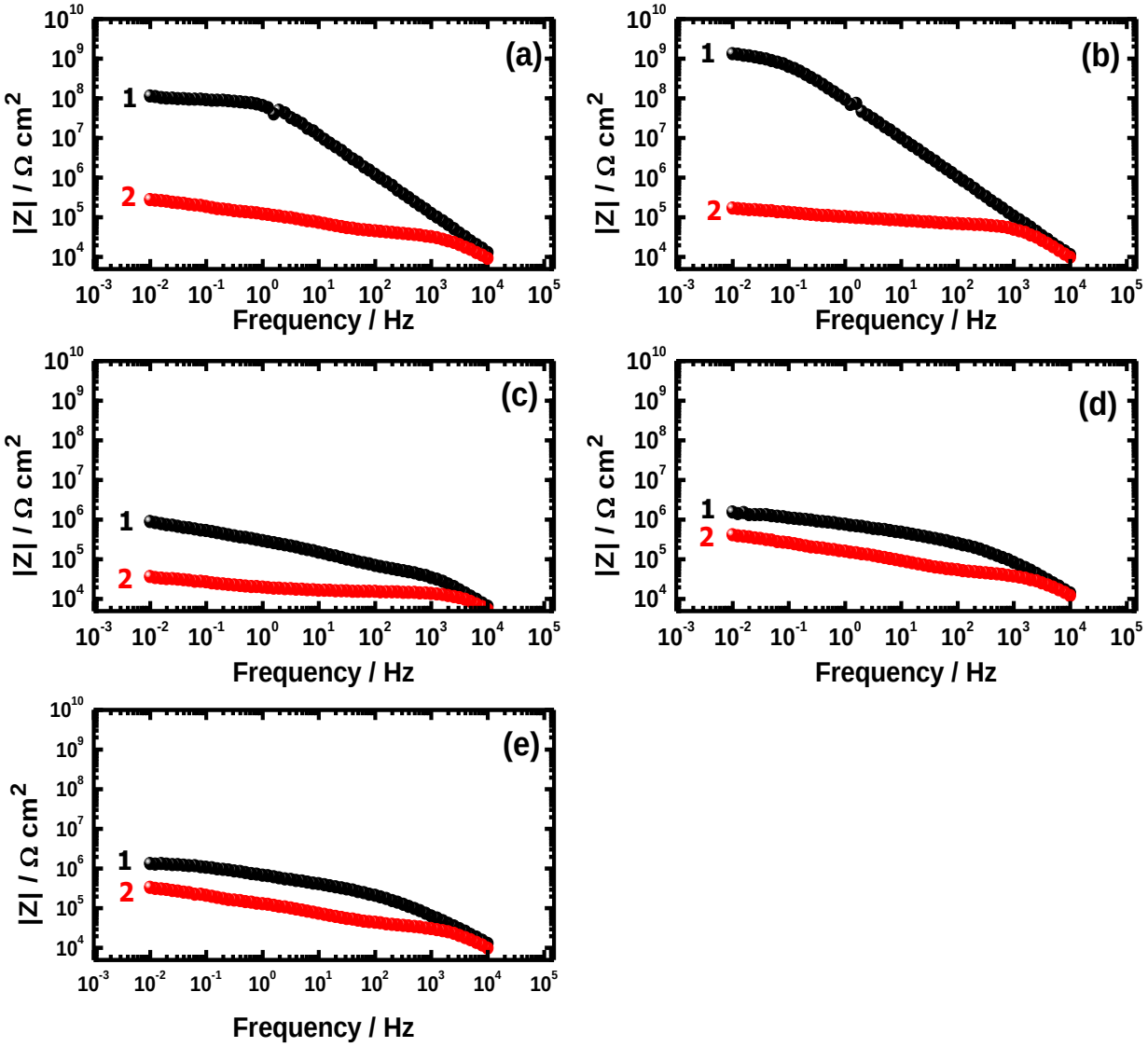

Figure 8. Bode impedance plots for the epoxy coatings, (a) F-1, (b) F-2, (c) F-3, (d) F-4, and (e) F-5 after their immersion for (1) 60 min and (2) 7.0 days, respectively in freely aerated 0.6 M NaCl solutions.

On the other hand and after 7.0 days immersion, Fig. 6, the size of the diameter of the semicircle as well as the segment decreased for all coated samples compared to its behavior after 60 min exposure time. This is due to the degradation of coatings with time, which allows the corrosive ions from the test solution to attack the weak and flawed parts on the surface of the coated steel coupons and cause its corrosion [1,4]. Liu et al. [30] reported that the corrosion of coated metal substrate takes place as a result of the diffusion of the corrosive chloride ions into the coating/metal interface upon immersing the coated metal in the corrosive solution i.e. invasive penetration of the corrosive electrolytes. Ramezanzadeh and Attar [31] have reported also that the diffusion of the

corrosive ions into the surface of the epoxy coated metallic coupons is attributed to the presence of nonreacted epoxide groups remain in the system and the hydrolytic degradation can be responsible for the breakdown of etheric linkages causing electrolyte diffusion. Fig. 6 and Table 3 thus confirm that the corrosion resistance of the epoxy coated steel coupons decreases, which is opposite to degradation, in this order; F-5 > F-4 > F-1 > F-2 > F-1. This was also supported by the decrease of R_S, R_{p1}, and R_{p2} values and increase of Y_{Q1} and Y_{Q2} ones in the same order.

Table 3. EIS parameters obtained by fitting the EIS data for the various fabricated epoxy coatings that had been immersed in 0.6 M NaCl solutions for 60 min and 7.0 days, respectively.

Sample	EIS Parameter						
	R_S / Ω cm^2	Q_1		R_{P1} / kΩ cm^2	Q_2		R_{P2} / kΩ cm^2
		Y_{Q1}/ µF cm^{-2}	n_1		Y_{Q2}/ µF cm^{-2}	n_2	
F-1 (60 min)	1625	0.00021	0.98	1887	0.97	0.43	1257
F-2 (60 min)	1648	0.00018	0.98	2307	0.054	0.44	1648
F-3 (60 min)	1312	0.00023	1.0	512	1.6	0.36	463
F-4 (60 min)	1940	0.00035	0.89	1212	0.65	0.30	618
F-5 (60 min)	2011	0.00155	0.76	1244	0.78	0.29	741
F-1 (7.0 days)	1419	0.00017	1.0	225	4.69	0.33	175
F-2 (7.0 days)	1552	0.00016	0.8	479	1.032	0.22	327
F-3 (7.0 days)	1213	0.00395	0.76	99	2.26	0.32	109
F-4 (7.0 days)	1865	0.00013	0.8	982	3.41	0.34	271
F-5 (7.0 days)	1932	0.00015	0.76	1131	0.76	0.29	239

In order to confirm the EIS Nyquist spectra for the different fabricated epoxy coatings, the Bode impedance spectra were also plotted. Fig. 8 shows Bode impedance plots for the epoxy coatings, (a) F-1, (b) F-2, (c) F-3, (d) F-4, and (e) F-5 after their immersion for (1) 60 min and (2) 7.0 days, respectively in freely aerated 0.6 M NaCl solutions. It is clearly seen from Fig. 8 that the impedance of the interface (|Z|) for all the fabricated epoxy coatings increased with decreasing frequency. These plots confirmed that |Z| recorded higher values overall the whole frequency range for all the epoxy coatings after 60 min immersion in the chloride test solution and its values for F-2 sample showed the highest impedance value. Moreover, increasing the immersion time to for 7.0 days decreased the values of |Z| against frequency for all samples, which is due to the degradation of coatings with time. It is also seen that the highest increase for |Z| with frequency after 7.0 days immersion was for the formula F-5, which agrees with the conclusion obtained from Nyquist plots at the same conditions. It has been reported [4,29] that the increase of |Z| particularly at the low frequency region increases the passivation of the surface against corrosion.

4. CONCLUSIONS

In the present investigation, we fabricated five different epoxy coatings by physical mixing different stoichiometry variations of BBERA epoxy coating with PAA-115 curing agent at ambient temperature. FT-IR was used to characterize the molecular composition for the glass coated with the fabricated epoxies. The thermal degradation and mechanical properties as well as the corrosion behavior after 60 min and 7.0 days immersion in 0.6 M sodium chloride solution for all the fabricated epoxy coatings were reported. The cross hatch tester, pendulum hardness, mandrel bend, and scratch tester measurements indicated that the fabricated epoxy coatings have excellent mechanical properties. EIS data proved that the epoxy formulas have high corrosion resistance, Rp, when the measurements were collected after 60 min immersion in 0.6 M NaCl solution; the highest Rp value was recorded for the sample with +10 stoichiometric variation between BBERA and PAA-115. On the other hand, increasing the immersion time to 7.0 days decreased the corrosion resistance for all formulas due to the degradation of coatings by the corrosive chloride ions presented in the test solution. Results collectively indicated that the five fabricated coatings provide high thermal stability, excellent mechanical properties and good corrosion resistance in 0.6 M NaCl solutions.

ACKNOWLEDGEMENTS
The authors are very grateful to the Saudi Arabian Oil Company (Saudi ARAMCO) and the Center of Excellence for Research in Engineering Materials (CEREM) for the financial support.

References

1. M. A. Alam, El-Sayed M. Sherif, S. M. Al-Zahrani, *Int. J. Electrochem. Sci.* 8 (2013) 3121.
2. S. C. Tjong, H. Chen, *Mater. Sci. Eng. R,* 45 (2004) 1.
3. L. Maya, W.R. Allen, A. L. Glover, J. C Mabon, *J. Va. Sci. Technol. B,* 13 (1995) 61.
4. M. A. Alam, El-Sayed M. Sherif, S. M. Al-Zahrani, *Int. J. Electrochem. Sci.* 8 (2013) 8388.
5. S. Veprek, A. S. Argon, *Surf. Coat. Technol.,* 146–147 (2001) 175.
6. F. Vaz, L. Rebouta, *Mater. Sci. Forum*, 383 (2002) 143.
7. Z.-M. Huanga, Y.-Z. Zhang, M. Kotakic, S. A. Ramakrishna, *Composite Sci. Technol*., 63 (2003) 2223.
8. V. Provenzano, R. L. Holtz, *Mater. Sci. Eng. A,* 204 (1995) 125.
9. Abid Karim, *The Scientific World J.,* 2013 (2013) Article ID 928062, 3 pages.
10. A. Talo, P. Passiniemi, O. Forsén, S. Yläsaari, *Synthetic Metals,* 85 (1997) 1333.
11. P. Kalenda, *Pigment & Resin Technol.,* 30 (2001) 150.
12. J. E. Gray, B. Luan, *J. Alloys Compud.,* 336 (2002) 88.
13. F. A. Lowenheim, *Modern Electroplating,* John Wiley and Sons Inc: New York, USA, 1974.
14. F. W. Eppensteiner, M. R. Jenkins, *Metal Finishing Guidebook and Directory,* 90 (1992) 413.
15. D. Perreux, C. Suri, *Composite Sci. Technol*., 57 (1997) 1403.
16. B. Wetzel, F. Haupert, M. Qiu Zhang, *Composite Sci. Technol*., 63 (2003) 2055.
17. El-Sayed M. Sherif, M. Es-saheb, A. A. Elzatahry, E. kenawy, A. S. Alkaraki, *Int. J. Electrochem. Sci.* 7 (2012) 6154.
18. M. Es-saheb, El-Sayed M. Sherif, A. A. Elzatahry, M. M. El Rayes, A. K. Khalil, *Int. J. Electrochem. Sci.* 7 (2012) 10442.
19. E. M. Sherif, S.-M. Park, *J. Electrochem. Soc.,* 152 (2005) B428.

20. N. B. Colthup, L. H. Daly, S. E. Wiberley, *Introduction to Infrared and Raman Spectroscopy*, 3rd ed., Academic Press, San Diego, CA, 1990.
21. G. Socrates, *Infrared Characteristic Group Frequencies Tables and Charts*, 3rd ed., Wiley & Sons Inc., New York, 2004.
22. A. Bhattacharya, J. W. Rawlins, P. Ray, *Polymer grafting and crosslinking*, New Jersey, John Wiley & Sons Inc. 2009.
23. El-Sayed M. Sherif, A. H. Ahmed, *Synthesis and Reactivity in Inorganic, Metal-Organic, and Nano-Metal Chemistry*, 40 (2010) 365.
24. El-Sayed M. Sherif, *J. Mater. Eng. Perform.* 19 (2010) 873.
25. El-Sayed M. Sherif, *J. Solid State Electrochem.*, 16 (2012) 891.
26. El-Sayed M. Sherif, *Mater. Chem. Phys.*, 129 (2011) 961.
27. A. K. Khalil, El-Sayed M. Sherif, A. A. Almajid, *Int. J. Electrochem. Sci.* 6 (2011) 6184.
28. El-Sayed M. Sherif, A. A. Almajid, *Int. J. Electrochem. Sci.* 6 (2011) 2131.
29. F.H. Latief, El-Sayed M. Sherif, A.A. Almajid, H. Junaedi, *J. Anal. Appl. Pyrolysis*, 92 (2011) 485.
30. J. Liu, F. Wang, K. C. Park, *Mater. Corros.* 62 (2011) 1008.
31. B. Ramezanzadeh, M. M. Attar, *Prog. Org. Coat.*, 71 (2011) 314.